

# UCLA

## UCLA Previously Published Works

### Title

A GCase Chaperone Improves Motor Function in a Mouse Model of Synucleinopathy

### Permalink

<https://escholarship.org/uc/item/2pp460nv>

### Journal

Neurotherapeutics, 11(4)

### ISSN

1933-7213

### Authors

Richter, Franziska  
Fleming, Sheila M  
Watson, Melanie  
[et al.](#)

### Publication Date

2014-10-01

### DOI

10.1007/s13311-014-0294-x

Peer reviewed

# A GCCase Chaperone Improves Motor Function in a Mouse Model of Synucleinopathy

Franziska Richter · Sheila M. Fleming · Melanie Watson · Vincent Lemesre · Lee Pellegrino · Brian Ranes · Chunni Zhu · Farzad Mortazavi · Caitlin K. Mulligan · Pedrom C. Sioshansi · Sindalana Hean · Krystal De La Rosa · Richie Khanna · John Flanagan · David J. Lockhart · Brandon A. Wustman · Sean W. Clark · Marie-Françoise Chesselet

Published online: 20 July 2014

© The American Society for Experimental NeuroTherapeutics, Inc. 2014

**Abstract** Mutation of the lysosomal hydrolase acid- $\beta$ -glucosidase (GCCase), which leads to reduced GCCase activity, is one of the most frequent genetic risk factors for Parkinson's disease (PD) and promotes  $\alpha$ -synuclein accumulation in the brain, a hallmark of PD and other synucleinopathies. Whether targeting GCCase pharmacologically is a valid therapeutic strategy for sporadic PD in the absence of GCCase mutation is unknown. We have investigated whether increasing the stability, trafficking, and activity of wild-type GCCase could be beneficial in synucleinopathies by administering the pharmacological chaperone AT2101 (afegostat-tartrate, isofagomine) to mice that overexpress human wild-type  $\alpha$ -synuclein (Thy1-aSyn mice). AT2101 administered orally for 4 months to Thy1-aSyn mice improved motor and nonmotor function, abolished microglial inflammatory response in the substantia nigra, reduced  $\alpha$ -synuclein immunoreactivity in nigral dopaminergic neurons, and reduced the number of small  $\alpha$ -synuclein aggregates, while increasing the number of large  $\alpha$ -synuclein aggregates. These data support the further investigation of pharmacological chaperones that target GCCase as a therapeutic approach for sporadic PD and other synucleinopathies, even in the absence of glucocerebrosidase mutations.

**Keywords** Parkinson's disease · Alpha-synuclein · Acid- $\beta$ -glucosidase · Mouse model · Chaperone · Motor behavior

## Introduction

Multiplication of the  $\alpha$ -synuclein gene causes familial Parkinson's disease (PD), and polymorphisms increase the risk of sporadic PD [1, 2], which is the most frequent being synucleinopathy [3]. Mutations in *GBA1*, the gene for the lysosomal hydrolase acid  $\beta$ -glucosidase (GCCase), are the most common known genetic risk factor for PD [4, 5]. Mutations in *GBA1* reduce the stability of GCCase, favoring premature degradation by the endoplasmic reticulum (ER)-associated protein degradation pathway, reduction of the lysosomal activity of GCCase, or both. In turn, these deficits in GCCase can lead to increased accumulation of  $\alpha$ -synuclein in the central nervous system (CNS), a protein central to PD pathology [6]. This feed-forward pathological loop between mutant GCCase and  $\alpha$ -synuclein provides a mechanism for the increased risk for PD among carriers of mutant *GBA1* alleles [6–8]. A parallel mechanism may occur in patients without the Gaucher mutation, involving the formation of an  $\alpha$ -synuclein and GCCase complex that inhibits enzyme function [9]. Furthermore, wild-type (WT) GCCase and  $\alpha$ -synuclein interact preferably at lysosomal pH, suggesting a beneficial effect of lysosomal GCCase on  $\alpha$ -synuclein degradation [10], which could be deficient as a result of the formation of the  $\alpha$ -synuclein and GCCase complex. These data suggest that GCCase deficiency may also play a role in sporadic PD, and, indeed, a loss of GCCase activity and protein has been recently reported in the substantia nigra (SN) of some patients with sporadic PD without *GBA1* mutation [11]. Overexpressing GCCase reduced the accumulation and aggregation of  $\alpha$ -synuclein, and improved neuronal function

F. Richter · S. M. Fleming · M. Watson · V. Lemesre · C. Zhu · F. Mortazavi · C. K. Mulligan · P. C. Sioshansi · S. Hean · K. De La Rosa · M.-F. Chesselet (✉)  
The David Geffen School of Medicine at UCLA, 710 Westwood Plaza, Los Angeles, CA 90095-1769, USA  
e-mail: MChesselet@mednet.ucla.edu

L. Pellegrino · B. Ranes · R. Khanna · J. Flanagan · D. J. Lockhart · S. W. Clark  
Amicus Therapeutics, 1 Cedar Brook Drive, Cranbury, NJ 08512, USA

B. A. Wustman  
Amicus Therapeutics, 11099 North Torrey Pines Road, La Jolla, CA 92037, USA

[12, 13], validating GCCase as a therapeutic target for synucleinopathies [14]. Taken together, these observations suggest that therapeutic interventions that increase GCCase stability and activity in the lysosome may represent a new therapeutic approach to break the cycle of  $\alpha$ -synuclein accumulation in synucleinopathies such as PD [7, 14].

Pharmacological chaperones are orally available small molecules that can access the CNS, bind and stabilize their target protein, and increase GCCase activity in the brain without direct administration to the CNS [14, 15]. The pharmacological chaperone AT2101 (afegostat-tartrate, isofagomine) specifically and reversibly binds GCCase in the ER with high affinity; this stabilizes the active form of the enzyme in the ER and increases trafficking of GCCase to lysosomes [16, 17]. The low pH of lysosomes is optimal for the activity and stability of GCCase, and reduces its affinity for AT2101 (Fig. 1a) [16, 17]. Because GCCase is less stable in the near-neutral pH of the ER [19], even WT GCCase is subject to degradation by the ER quality control system and AT2101 can further stabilize WT GCCase.

The goal of the present study was to assess the ability of the orally available pharmacological chaperone for GCCase, AT2101, to improve the behavioral and pathological deficits induced by  $\alpha$ -synuclein overexpression in the absence of GCCase deficiency. This is a critical step in order to support future studies of this approach for the treatment of sporadic PD patients without *GBA1* mutations. We utilized a mouse model in which human WT  $\alpha$ -synuclein is overexpressed under the murine Thy-1 promoter (Thy1-aSyn) in the absence of mutations in GCCase [20–24]. The administration of AT2101 increased GCCase activity in brain, indicating target engagement, and resulted in improved motor deficits and reduced neuropathology associated with this synucleinopathy model.

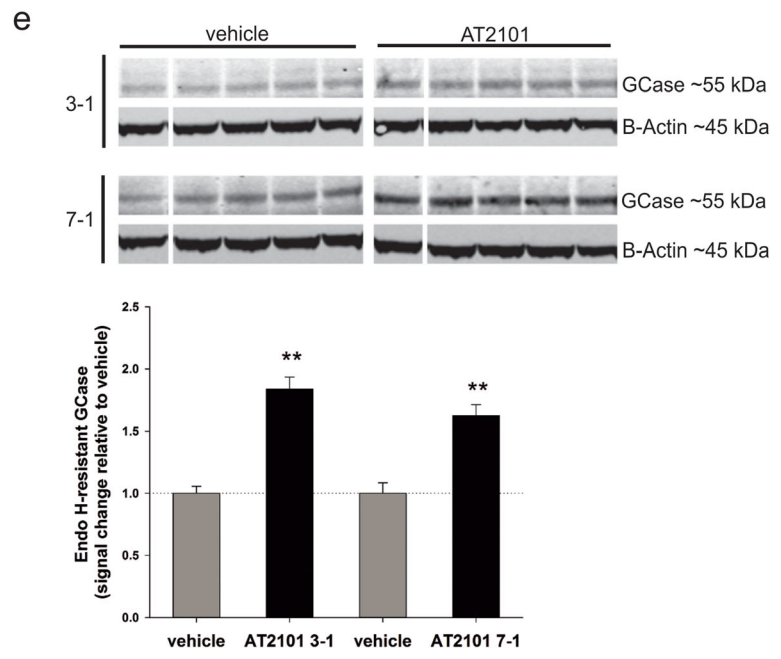
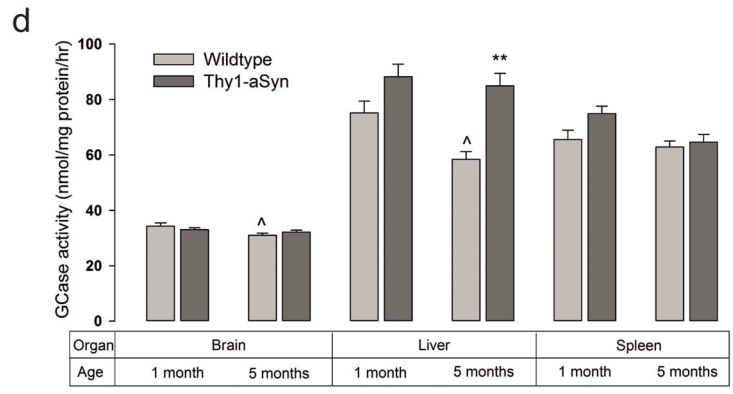
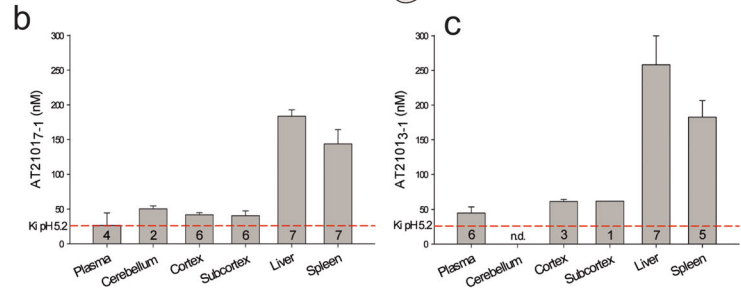
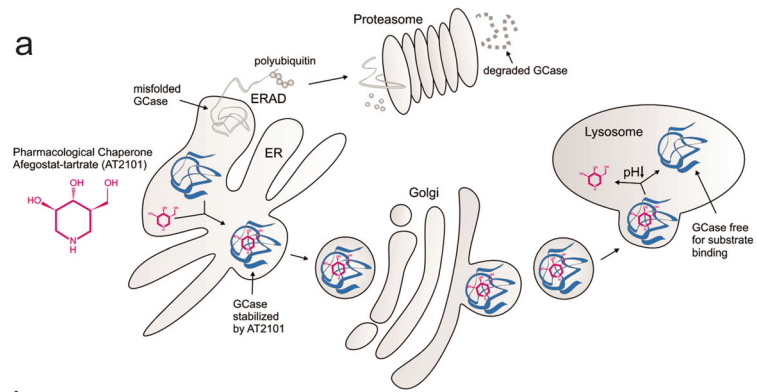
## Materials and Methods

### Animals and Experimental Design

Animal care was conducted in accordance with the United States Public Health Service Guide for the Care and Use of Laboratory Animals, and procedures were approved by the Institutional Animal Care and Use Committee at the University of California Los Angeles (UCLA). Male transgenic mice overexpressing human WT  $\alpha$ -synuclein under the Thy-1 promoter (Thy1-aSyn) were developed previously [21]. One hundred and fifty-two male mice from 48 litters were included in the study. Five mice were euthanized prior to the end of the study owing to unrelated health issues (e.g., tooth abscess). Control animals were littermates of Thy1-aSyn mice. Mice were genotyped at 10 days of age using polymerase chain reaction from tail samples or fecal pellets, and assigned to a study group, whereby mice from the same litter were

**Fig. 1** GCCase activity and AT2101 effects in human wild-type (WT)  $\alpha$ -synuclein (Thy1-aSyn) mice. **a** Mechanism of action for the pharmacological chaperone AT2101. GCCase is a lysosomal hydrolase with optimal stability and activity in the low pH environment of lysosomes. In the near-neutral pH of the endoplasmic reticulum (ER) where GCCase initially folds into its tertiary structure, the protein is not as stable as in lysosomes; as a result, a fraction of the synthesized protein is subject to degradation by the ER quality control system. AT2101 binding to GCCase in the ER stabilizes GCCase, allowing passage through ER quality control and increased trafficking to lysosomes. Once in lysosomes, a combination of factors makes GCCase more accessible to its substrates: the reversible nature of the binding and dissociation of AT2101, competition of the natural substrates with AT2101, and the low pH that favors dissociation of AT2101. The net result is an increase in lysosomal GCCase activity even in the presence of pharmacological chaperones such as AT2101. Note that the small molecule AT2101 (147 Da) and the enzyme GCCase (60 kDa) are not drawn to scale. ERAD=endoplasmic reticulum-associated protein degradation. **b, c** AT2101 levels were monitored in tissues of 1-month-old Thy1-aSyn mice after a continuous treatment over **b** 7 or **c** 3 days followed by a 24-h washout. All tissues had AT2101 levels above the  $K_i$  (inhibition constant of AT2101 towards WT GCCase at pH 5.2=26 nM) after the 24-h washout, consistent with the need for a washout period (either 4 or 7 days “off”) to provide a period in which GCCase is unencumbered by AT2101 inhibition. Bars represent the mean of the group+SEM ( $n=7$  mice per group); only values with detectable AT2101 concentration are shown (“n” number in column); duplicate measurements were done for each tissue and mouse; n.d. = not determined owing to insufficient tissue availability. **d** GCCase activity in brain, liver, and spleen from 1- or 5-month-old WT and Thy1-aSyn mice not administered AT2101 (baseline). Interestingly, 5- but not 1-month-old Thy1-aSyn mice had increased GCCase activity in the liver compared with WT mice. Furthermore, we found a slight decrease in GCCase activity with age in brain and liver, which reached significance in WT mice only.  $**p<0.01$  vs WT,  $^{\wedge}p<0.05$  vs 1 month,  $2 \times 2$  analysis of variance, Bonferroni  $t$  test, mean+SEM ( $n=6-10$  mice per group), measurements done in duplicate for each sample. Fold changes after AT2101 administration are shown in Table 2. **e** Quantity of endoglycosidase H (EndoH)-resistant GCCase extracted from subcortex (brain tissue after dissection of cortex and cerebellum, consisting mostly of striatum, hippocampus, and thalamus) of 1-month-old Thy1-aSyn mice administered vehicle or AT2101 (3-on/1-off or 7-on/1-off) monitored via Western blotting, indicative of GCCase that has trafficked beyond the ER and reached the mid-Golgi apparatus [18]. To enable a comparison of changes in GCCase levels between the 2 regimens, each value was normalized to the mean value of the respective 5 vehicle animals of the regimen. Images of blots for GCCase and beta-actin loading control, data as mean+SEM ( $n=5$ ),  $**p<0.01$  compared with vehicle; no significant differences between 3 and 7 days administration (Student’s  $t$  test)

distributed across vehicle and drug groups. Therefore, mice from different study groups were always administered, tested and analyzed in parallel until all groups were filled to the predetermined group sizes. Group sizes were determined based on our power analysis [24]. Final group sizes were 14–19 mice, which provided sufficient power for all tests performed. Data analysis was performed with all data at the end of the study, when all groups were filled to final size (given in detail in each table or figure legend). No animals were excluded from analysis as, based on Grubbs test for outliers, there were no statistical significant outliers. Genotype was verified at the end of the study. AT2101 (provided by Amicus Therapeutics) was dissolved in drinking water (vehicle). Mice had continuous and



ad libitum access to the water or water with AT2101. Water intake was measured to verify similar and expected daily intake in both vehicle and AT2101 study groups.

Three different cohorts were examined. First, for baseline GCCase activity, 1-month-old Thy1-aSyn mice and their WT littermates were used without drug administration ( $n=10$ ). Second, for pharmacokinetic/pharmacodynamic studies, Thy1-aSyn mice were administered AT2101 at 100 mg/kg free base equivalent or vehicle in drinking water for 3 or 7 days followed by a 1-day vehicle-only washout ( $n=7$  per group). Third, for efficacy studies, eight cohorts of mice (4 WT and 4 Thy1-aSyn,  $n=14-19$  each) were administered AT2101 at 100 mg/kg free base equivalent or vehicle in drinking water starting a 1 month of age for 4 months. Because of their mechanism of action, schedules of administration of pharmacological chaperones are designed to balance periods of stabilization and inactivation (while the chaperone concentration is high in brain) and periods of enzymatic activity (while chaperone concentration is low), thus requiring a succession of “on” and “off” periods of drug administration. The regimens used in this study were chosen to maximize the drug benefits on enzymatic activity without attempting to administer equivalent doses to the animals. Specifically, 2 different regimens were used: 3 days of AT2101 at 100 mg/kg free base equivalent followed by 4 days with vehicle only (3-on/4-off); and 7 days of AT2101 administration followed by 7 days with vehicle only (7-on/7-off). A final washout period of 7 days followed the last day of drug administration for both regimens before euthanasia in order to compare effects of both regimens on pathology and postmortem measurements.

General condition, body weight, and body temperature (using a rectal temperature probe; Stoelting, Wood Dale, IL, USA) were recorded biweekly over the administration period. Animals were maintained on a reverse light/dark cycle with lights off at 10:00 AM and all testing was performed between 12:00 and 4:00 PM during the dark cycle under low light. Drug administration, data collection, and data analyses were performed by investigators blinded to treatment and genotype. The investigator preparing the water bottles containing water or water with AT2101 was not involved in behavioral testing, data collection, or analysis. Genotype of mice was not indicated on cage cards.

#### AT2101 and GCCase Measurements

AT2101 concentration was determined in plasma, brain (cerebellum, cortex, remaining brain tissue (“subcortex”), liver, and spleen using liquid chromatography–mass spectrometry/mass spectrometry.

Tissue GCCase activity was measured as described with slight modifications [16]. Tissue lysates were prepared by homogenizing tissue in McIlvaine buffer (100 mM sodium citrate, 200 mM sodium phosphate dibasic, 0.25 % sodium

taurocholate, and 0.1 % Triton X-100, pH 5.2). Total protein was determined in lysates using the BCA protein assay (Pierce, Rockford, IL, USA).

GCCase trafficking out of the ER was monitored by examining N-glycan carbohydrate processing via Western blotting [18]. Samples were either undigested or treated with EndoH or PNGaseF. Left subcortical tissue was homogenized in 25 mM Bis-Tris, pH 6.5, 150 mM NaCl, 0.1 % Triton-X100 with Complete Protease Inhibitor Cocktail (Roche, Indianapolis, IN, USA) using a rotostat. Cleared supernatants were treated with endoglycosidase according to the manufacturer’s instructions (New England Biolabs, Ipswich, MA, USA). The glycoforms were separated by sodium dodecyl sulfate polyacrylamide gel electrophoresis and transferred to nitrocellulose. GCCase was visualized by anti-GCCase antibody (Sigma-Aldrich G4171; St. Louis, MO, USA), and anti- $\beta$ -actin (Sigma-Aldrich A5441) was used as a loading control. The blot was analyzed using IRDye secondary antibodies and infrared scanner technology (LiCor, Lincoln, NE, USA).

#### Behavioral Testing

Motor behavior was measured during drug administration in the final (fourth) month of AT2101 administration with the pole, challenging beam, and cylinder tests carried out as described previously [20]. For the pole and beam tests, animals were trained for 2 days and recorded on the third day for 5 trials. For the cylinder test, mice were recorded for 3 min without prior training. Olfactory testing was performed 1 week after motor behavior using the buried pellet test as described previously [25].

#### Euthanasia, Histology, and Quantification

Mice were sacrificed 7 days after the end of AT2101 administration in order to enable direct comparison of effects on GCCase activity and  $\alpha$ -synuclein pathology in the absence of high compound concentrations in brain. A subset of mice from each group assigned at the beginning of the study was sacrificed by decapitation and used for GCCase measurement. The other mice were perfused with 4 % paraformaldehyde for histological analysis of brain sections using different primary antibodies for immunohistochemistry (Table 1). For  $\alpha$ -synuclein and tyrosine hydroxylase (TH) co-labeling of nigral sections, secondary antibodies were conjugated with Alexa 488 ( $\alpha$ -synuclein) and Alexa 594 (TH). For assessment of  $\alpha$ -synuclein aggregates, sections were treated with Proteinase K as described previously [26–28]. Microglial activation was quantified in a blinded fashion in one section of the SN ( $n=5$  mice/genotype).

To measure  $\alpha$ -synuclein staining in dopaminergic (DA) nigrostriatal neurons, immunofluorescence double-labeled images from the SN were acquired at 40 $\times$  using the tile scan

**Table 1** Primary Antibodies

Antigen	Antibody	Source	Concentration
$\alpha$ -Synuclein	Mouse antihuman and mouse- $\alpha$ -synuclein; clone 42	BD Biosciences, San Jose, CA	1:500
Ionized calcium binding adaptor molecule 1 (IBA-1)	Polyclonal rabbit anti-Iba1	Wako Pure Chemical Industries Ltd., Osaka, Japan	1:500
Tyrosine hydroxylase (TH)	Rabbit anti-TH	Millipore, Billerica, MA, USA	1:600
Glial fibrillary acidic protein (GFAP)	Polyclonal rabbit anti-GFAP	Dako, Glostrup, Denmark	1:400

function of the Leica Application Suite for Advanced Fluorescence and a Leica (Buffalo Grove, IL, United States) TCS SP5 MP-STED microscope. The laser intensity, confocal aperture, photomultiplier tube (PMT) voltage, offset, electronic gain, scan speed, image size, and zoom were set using a control section and kept consistent throughout the entire experiment. Fluorescence intensity for  $\alpha$ -synuclein immunoreactivity was measured in all TH-positive neurons of the SN that were in focus in one section per animal using Image J software (v1.45; National Institutes of Health, Bethesda, MD, USA). Specifically, in the SN pars compacta of both hemispheres, each TH-positive neuron with a nucleus was identified and outlined, excluding the nucleus from the area to be measured.  $\alpha$ -Synuclein immunofluorescence intensity measurements were collected for individual TH-positive neurons using Image J software. To account for differences in background staining intensity, intensity measurements of an area lacking TH-positive or  $\alpha$ -synuclein-positive cells or processes (cerebral peduncle) were taken from each section and fluorescence intensities were subtracted from the measured immunofluorescence intensity of each individual neuron, resulting in the final intensity values. There were no differences in background staining intensities between vehicle-treated and AT2101-treated mice.

For the quantification of  $\alpha$ -synuclein fluorescent immunolabeling in brain regions, images of immunofluorescence-labeled sections were acquired using an Agilent (Santa Clara, CA, United States) microarray scanner equipped with a krypton/argon laser (647 nm) at 10  $\mu$ m resolution with the photomultiplier tube set at 5 % [29], and immunofluorescence intensity was measured with ImageJ in the region of interest.

Quantitative analysis of proteinase K-resistant  $\alpha$ -synuclein aggregate number, surface occupied by aggregates, and aggregate size distribution was performed in the SN. One section from the SN immunostained for  $\alpha$ -synuclein with proteinase K was used per animal. Quantification was only performed on tissue from Thy1-aSyn mice because WT mice do not develop proteinase K-resistant aggregates of  $\alpha$ -synuclein [26]. The contour of the SN was delineated at 5 $\times$  objective using StereoInvestigator software coupled to a Leica DM-LB microscope with a Ludl XYZ motorized stage. The contour was then divided into 2 subregions, largely corresponding to the

SN pars compacta and to the SN pars reticulata, respectively (see Fig. 6a). Two images from 2 different areas in each subregion of the SN were then acquired using the same software and 40 $\times$  objective (1 image per subregion). Images of the SN from both hemispheres were transformed to 8-bit files using ImageJ. For particle analysis in ImageJ the threshold was set manually to ensure the inclusion of all aggregates ranged from 1  $\mu$ m to 30  $\mu$ m. The inclusions were defined by circularity to avoid inclusion of dust or other artifacts. The surface area covered by aggregates was measured and the number of aggregates was calculated per 100  $\mu$ m<sup>2</sup>.

Microglia were identified by immunostaining with IBA-1, and the analysis of their diameter was performed with the StereoInvestigator software (MicroBrightField, Colchester, VT, USA) as described previously [30]. Briefly, images were acquired at 40 $\times$  on a Leica DM-LB microscope with a Ludl XYZ motorized stage and z-axis microcator (MT12; Heidenheim, Traunreut, Germany). Morphologically distinct classes of IBA-1-positive cells could be distinguished as follows: resting ramified microglia had mean cell body diameters of 1–4  $\mu$ m, hyper-ramified microglia/partially activated microglia had mean cell body diameters of 5–6  $\mu$ m, and fully activated amoeboid microglia had mean cell body diameters of 7–13  $\mu$ m. Glial fibrillary acidic protein-positive astroglia in the SN were assessed qualitatively using a scoring system.

#### Quantification of $\alpha$ -Synuclein via Enzyme-linked Immunosorbent Assay

Human  $\alpha$ -synuclein levels were determined with a commercially available enzyme-linked immunosorbent assay (ELISA; Covance, Princeton, NJ, USA) following the manufacturer's protocol. Protein content of the homogenates was determined by BCA assay (Pierce).

#### Statistics

Analysis of variance (ANOVA) was used for multicomparisons. Bonferroni *t* test was used post hoc for pairwise comparison only if ANOVA returned significance for factors tested. Data were tested for equal variances prior to ANOVA. Mann–Whitney *U* test was used for nonparametric comparisons.  $\chi^2$  or Fisher's exact test were used for analysis

of contingency tables. The null hypothesis was rejected at a  $p$ -value of 0.05 (SigmaPlot 12; Systat Software, San Jose, CA, USA). For distribution analysis we used a bootstrapping method similar to a Kolmogorov–Smirnov test using custom MATLAB functions [30, 31]. The comparison was considered to be significant at the  $p < 0.05$  level when the sample parameter fell outside of the 95 % confidence interval of the control group, independent of assumptions about the probability distribution.

## Results

### AT2101 Increases GCase Trafficking and Activity in Brain

AT2101 stabilizes GCase and increases its trafficking to lysosomes (Fig. 1a) [17]. Lysosomal pH favors dissociation of AT2101 resulting in a net increase of lysosomal GCase activity [17]. Because the half-life of GCase greatly exceeds the half-life of AT2101, an extended “off” period without AT2101 provides additional GCase enzyme activity without inhibition from AT2101. To verify that AT2101 favored stabilization of GCase over enzyme inhibition *in vivo*, we initially determined AT2101 concentration and GCase activity in different organs and plasma after 3 or 7 days of compound administration in drinking water followed by 24 h washout (Fig. 1b, c; Table 2). After a 24-h washout, low-level AT2101 could be detected in plasma and tissues of Thy1-aSyn mice as expected, with no tissue having AT2101 levels more than 2.3-fold the  $K_i$  (Fig. 1b, c). Importantly, these compound levels resulted in the expected increase of GCase activity by 1.3–1.8-fold across different organs, including brain. We observed that the increase in GCase activity was larger after 7 days administration compared with 3 days, suggesting greater GCase levels during the “on” period (Table 2). In summary, our data confirm that AT2101 administration favored stabilization of GCase over enzyme inhibition when administered for 3 or 7 consecutive days. We also confirmed that increased GCase activity corresponds to increased trafficking beyond the ER by analysis of GCase glycosylation (Fig. 1e). Both the 7-on/1-off and the 3-on/1-off regimens increased trafficking about 1.7-fold. This supports that the additional GCase resulting from AT2101 administration is properly trafficked beyond the ER.

Next, we determined the level of endogenous GCase activity in our mouse model. Whole-brain GCase activity was similar between WT and Thy1-aSyn mice (Fig. 1d; Table 2). This confirmed that  $\alpha$ -synuclein overexpression did not hinder the ability of the chaperone to increase GCase activity, and that our model is suitable to assess the effects of increased GCase activity on pathology and motor dysfunction resulting from  $\alpha$ -synuclein accumulation in the absence of endogenous GCase alteration, a situation that is most similar to that of patients

with sporadic PD without *GBA1* mutations. Indeed, although a decrease in GCase activity has been reported in postmortem SN in PD, it is not clear that this occurs early in the disease and in all patients. Therefore, a conservative approach to evaluate the potential benefits of GCase chaperones in sporadic PD is to assess their effects in the context of normal levels of enzymatic activity. Similarly, lysosomally enriched fractions from Thy1-aSyn and WT brains revealed no differences in GCase activity (data not shown), likely reflecting the modest 3-fold overexpression of synuclein in Thy1-aSyn mice, in contrast to the reported decrease observed in neurons *in vitro* after an increase of  $\alpha$ -synuclein expression of 10-fold [8]. Such very high levels of  $\alpha$ -synuclein overexpression may be needed for effects on GCase activity. Differences in GCase trafficking cannot be excluded by our data and should be evaluated in Thy1-aSyn mice and compared with WT in future studies.

We verified that GCase activity was also increased in brain in the experimental animals used for behavioral and pathological studies after 4 months of administration of AT2101 (Table 2), confirming target engagement. In this case, measurements were made in the brains of mice that were sacrificed 7 days following 4 months of 7-on/7-off or 3-on/4-off drug administration to determine whether either regimen produced sustained elevation of GCase in brain. Both regimens produced significant and similar elevation of GCase in brain, confirming target engagement in both groups of mice in our study. These data confirmed that with the regimen used in this study, AT2101 increased GCase activity in brain after short- and long-term administration, and indeed the level of enzymatic activity was increased in brains of the animals examined behaviorally during the last month of AT2101 administration.

### AT2101 Improves Motor Function and Olfactory Deficits of Thy1-aSyn Mice

Although increased GCase activity is thought to be beneficial to offset the deficits induced by excess  $\alpha$ -synuclein [14], the magnitude of increase required for improvement is unknown. Furthermore, it is unclear whether different regimens of administration of the pharmacological chaperone produce similar effects *in vivo* on functional outcome. To determine whether the increase in GCase activity observed in our study was sufficient to reduce  $\alpha$ -synuclein-induced deficits, we examined the effects of both regimens on a range of motor deficits that are exhibited by the Thy1-aSyn mice [20]. These deficits, which are possibly due to dysfunction in nigrostriatal [22] or extranigral neuronal circuits [32, 33], are distinct from parkinsonism but provide evidence of *in vivo*, functional alterations resulting from  $\alpha$ -synuclein overexpression. Importantly, these deficits are established at an early age, and they are already quite large at the earliest age we have examined in this model (2–3 months of age [20]).

**Table 2** AT2101 increases GCCase activity in brain, liver, and spleen

Cohort	Genotype	Treatment	Regimen	GCCase activity Mean±SEM (fold change AT2101/vehicle)				
				Brain			Liver	Spleen
				Cortex	Subcortex	Cerebellum		
Cohort 1 naive	WT	Naive	–	34.4±1.1			75.2±4.3	65.6±3.4
	Thy1-aSyn			33.1±0.7			88.2±4.6	75.0±2.6
Cohort 2 kinetics/ dynamics	Thy1-aSyn/(1 month old)	Vehicle	7 days on drug, 1 day washout	51.2±2.5	56.0±3.5	51.6±1.8	141.2±9.5	108.9±2.3
		AT2101		92.3±2.3 (1.8)* <sup>†</sup>	88.5±6.1 (1.6)* <sup>‡</sup>	93.2±3.6 (1.8)* <sup>†</sup>	253.3±13.5 (1.8)* <sup>†</sup>	197.3±7.7 (1.8)* <sup>†</sup>
	Thy1-aSyn/(1 month old)	Vehicle	3 days on drug, 1 day washout	46.6±1.9	54.8±1.5	49.3±2.6	126.9±2.3	98.3±3.4
		AT2101		66.7±1.9 (1.4)*	72.4±4.5 (1.3)*	62.7±2.9 (1.3)*	181.3±9.6 (1.4)*	143.2±5.1 (1.5)*
Cohort 3 efficacy studies	WT (5 months old at sacrifice)	Vehicle	7 days on drug, 7 days off drug over 4 months (final washout 7 days after last “on” day)	29.9±1.0			55.0±4.6	66.0±2.8
		AT2101		38.5±1.1 (1.29)*			83.7±4.9 (1.52)*	74.6±3.7 (1.13) <sup>§</sup>
	Thy1-aSyn (5 months old at sacrifice)	Vehicle		32.8±0.7			80.4±6.3	65.3±5.3
		AT2101		39.8±1.2 (1.21)*			105.3±4.9 (1.31)*	63.5±2.3 (0.97)
	WT (5 months old at sacrifice)	Vehicle	3 days on drug, 4 days off drug over 4 months (final washout 7 days after last “on” day)	31.9±1.0			60.8±3.4	60.6±3.1
		AT2101		38.9±1.2 (1.22)*			85.1±4.7 (1.40)*	72.1±5.7 (1.19)
Thy1-aSyn (5 months old at sacrifice)	Vehicle		31.6±1.0			89.0±6.5	64.0±2.7	
	AT2101		39.0±1.1 (1.23)*			87.5±6.5 (0.98)	72.3±3.2 (1.13)	

WT=wild type; Thy1-aSyn=human wild-type  $\alpha$ -synuclein. GCCase activity in mean±SEM and fold changes of the mean after AT2101 administration compared with vehicle. Cohort 1 shows GCCase activity in naïve WT and Thy1-aSyn mice. In cohort 2, GCCase activity was measured in Thy1-aSyn mice after 7 or 3 days on drug followed by 1 day washout compared with respective vehicle. Fold changes in this cohort serve to estimate the increase of GCCase activity during the respective regimens used in cohort 3. Three days of administration increased GCCase activity by 40 %, whereas 7 days of administration increased GCCase activity by 80 %, supporting the expected dose and duration effect. Cohort 3 presents GCCase activity in the 3-on/4-off or 7-on/7-off administration regimen administered over 4 months followed by a 7-day washout period prior to tissue harvesting, to enable assessment of sustained effects on pathology under low drug concentrations. \* $p$ <0.01 AT2101 vs vehicle. <sup>†</sup> $p$ <0.01, 3 days vs 7 days of AT2101, <sup>§</sup> $p$ <0.05 AT2101 vs vehicle. <sup>‡</sup> $p$ <0.05, 3 days vs 7 days AT2101 2×2 analysis of variance, Bonferroni  $t$  test.  $n$ =6–10 per group, measurements obtained in duplicate for each sample

We assessed behavioral deficits on the pole and beam during the final month of drug administration. Thy1-aSyn mice take significantly longer time than WT mice to turn around (Fig. 2b) and to descend (Fig. 2c) the pole, a test of balance and coordination (Fig. 2a) [20]. Administration of 7-on/7-off AT2101 markedly reduced the deficit, resulting in a 30 % improvement over 5 trials (Fig. 2b, c). The number of mice able to perform the task within 60 s noticeably increased in Thy1-aSyn mice receiving 7-on/7-off AT2101 in trials 2–5 (Fig. 2d). No Thy1-aSyn mice could perform this task within the time range of WT mice in the absence of AT2101. However, 36 % of Thy1-aSyn mice that were administered 7-on/7-off AT2101 performed the task as fast as WT mice administered vehicle. Thus, 7-on/7-off AT2101 normalized the pole test behavior in a subset of Thy1-aSyn mice.

The challenging beam is an alternative test of speed and coordination, which is markedly impaired as early as 2 months of age in the Thy1-aSyn mice (Fig. 2e) [20]. Administration of AT2101 in the 7-on/7-off regimen decreased the time required by Thy1-aSyn mice to traverse the mesh-covered beam by 35 % (Fig. 2f). When administered vehicle, 41 % of Thy1-aSyn mice took longer than the slowest WT mouse to traverse the beam, whereas all but one of the Thy1-aSyn mice administered AT2101 performed as fast as WT mice. The decreased time to traverse the beam was not related to an increase in general activity (rearing) or stereotypic behavior (grooming), or to an improvement of hind limb movements observed in the cylinder test (Table 3). Furthermore, AT2101 decreased by 19 % the number of errors per step while traversing the beam (Fig. 2g). The 3-on/4-off regimen had a smaller effect than the 7-on/7-off regimen for reversing motor deficits (Tables 3



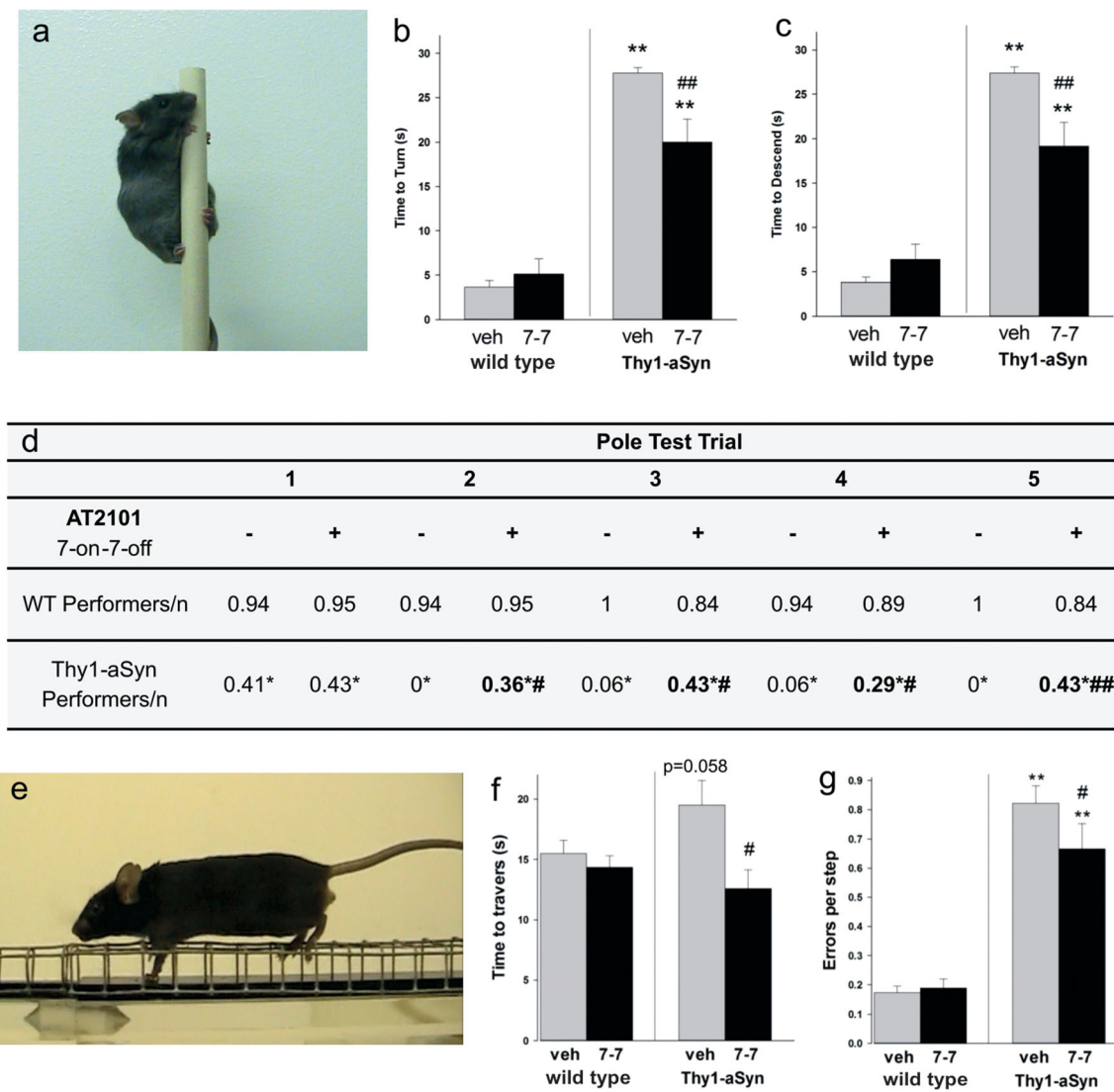


**Fig. 2** AT2101 7-on/7-off improved behavioral deficits. **a–g** Behavioral deficits in wild type (WT; vehicle=16; AT2101=19) and human wild-type (Wt)  $\alpha$ -synuclein (Thy1-aSyn) (vehicle=17; AT2101=14) mice administered AT2101 or water. **b** Time to turn and **c** time to descend as mean over 5 trials on the pole test [illustrated in (a)]. \*\* $p < 0.01$  compared with the respective WT; ## $p < 0.01$  compared with Thy1-aSyn Vehicle (mean+SEM, Mann–Whitney *U* test). There was no correlation of performance to body weight in Thy1-aSyn mice (Spearman Rank Order correlation,  $p > 0.05$ ). **d** Number of mice that were able to turn and

descend the pole (performers) as a ratio of the total number of mice per group. \* $p < 0.05$  compared with the respective WT (Fisher’s exact test); # $p < 0.05$ , ## $p < 0.01$  compared to the respective vehicle control (one-tailed Fisher’s exact test). **f** Time to traverse and **g** errors per step on the first trial on the challenging beam (mouse making an error on the grid is illustrated in (e)). \*\* $p < 0.01$  compared with the respective WT, # $p < 0.05$  or ## $p < 0.01$ , respectively, compared with Thy1-aSyn vehicle (mean+SEM, 2 $\times$ 2 analysis of variance followed by Bonferroni *t* test)

and 4) despite a similar effect on GCCase levels after 7 days washout at the end of the 4 months treatment. This suggests that the shorter “on” time over the course of treatment is less optimal than the longer “on” time afforded by the 7-on/7-off regimen, a possibility supported by our observation in the pilot study that 7-day administration of AT2101 produces a larger increase in GCCase activity than the 3-day administration (Table 2).

Thy1-aSyn mice also exhibit nonmotor deficits reminiscent of those present in PD patients [23, 24], notably a decrease in olfaction, an early and frequent deficit in PD [25]. We

subjected the mice to the buried pellet test, which has a high power to detect drug effects during the last month of drug administration [25]. The 7-on/7-off regimen of AT2101 showed only slight improvement of olfactory deficit in the fifth trial (Fig. 3; Table 3); however, the 3-on/4-off regimen produced a reduction (up to 32 %) in olfactory impairment (Fig. 3b; Table 4). These results are in agreement with the ability of the 3-on/4-off and the 7-on/7-off regimen to increase GCCase in brain (Table 2), and indicate that AT2101 administration can ameliorate nonmotor and motor deficits in the Thy1-aSyn mice. The difference in effects of the 2 regimens on various

**Table 3** Effect of AT2101 7-on/7-off on motor performance, spontaneous activity, and the surface pellet test

		WT				Thy1-aSyn						
		Vehicle		AT2101		Vehicle		AT2101				
Beam	Steps	18.69±0.62		17.26±0.56		16.35±0.58 <sup>†</sup>		16.57±0.43				
Activity	Rears	14.38±2.31		14.05±2.05		12.82±1.48		12.80±2.47				
	FL steps	49.00±5.14		74.05±6.12*		49.06±5.63		41.87±6.52				
	HL steps	36.69±4.52		55.00±5.67*		9.71±1.43 <sup>†</sup>		10.93±2.09 <sup>†</sup>				
	Groom	15.31±3.40		17.39±2.43		8.58±0.91		9.99±2.33‡				
	Olfaction	Visible pellet		7.82±1.66		8.34±2.04		12.02±3.01		8.34±2.23		
Olfaction test performance	Trial		1		2		3		4		5	
AT2101 7-on/7-off	-	+	-	+	-	+	-	+	-	+	-	+
WT performers/n	0.88	0.95	1	1	0.94	1	1	1	0.94	1	1	1
Thy1-aSyn performers/n	0.63	0.79	0.81	0.93	1	0.93	1	1	1	1	1	1

WT = wild type; FL = forelimb; HL = hindlimb; Thy1-aSyn = mice overexpressing human WT  $\alpha$ -synuclein. Challenging beam (steps on first trial), spontaneous activity in the cylinder test (rears, FL steps, HL steps, time spent grooming), visible (surface) pellet scores, and buried pellet performance [mice that found the buried food pellet in <300 s (performers) as ratio of the total number of mice per group] in Thy1-aSyn (vehicle=16, AT2101=16) and WT (vehicle=17, AT2101=14) mice administered vehicle or AT2101 in a 7-on/7-off regimen. \* $p$ <0.01 compared with WT mice administered vehicle (mean±SEM), and <sup>†</sup> $p$ <0.01 and <sup>‡</sup> $p$ <0.05 compared with the respective WT mice (2×2 analysis of variance for beam, activity and surface pellet; one-tailed Fisher's exact test for olfaction test performance)

behavioral deficits observed in the Thy1-aSyn mice suggest that different durations of “on” and “off” phases may produce

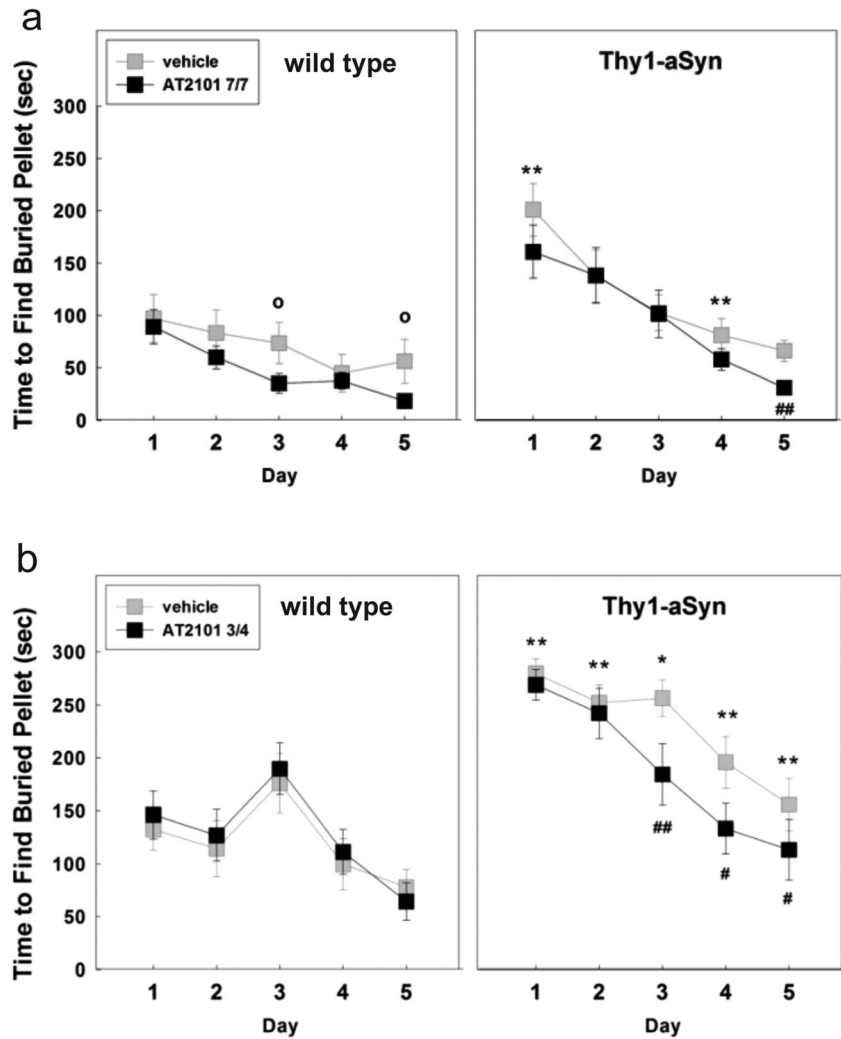
different increases in GCCase activity depending of the brain region and /or cell type.

**Table 4** Effect of AT2101 3-on/4-off on motor performance, spontaneous activity, and the surface pellet test

		WT				Thy1-aSyn						
		Vehicle		AT2101		Vehicle		AT2101				
Pole	Turn	4.31±1.68		3.80±1.75		24.51±2.52		25.60±2.42				
	Descend	4.01±1.54		5.20±1.69		23.61±2.88		24.98±2.70				
Beam	Time	13.81±1.41		13.16±1.43		15.66±1.16		17.22±1.48				
	Errors	0.10±0.02		0.10±0.02		0.51±0.05		0.55±0.07				
	Steps	17.33±0.38		16.69±0.51		16.00±0.45		15.75±0.57				
Activity	Rears	12.00±1.30		13.06±1.17		13.53±2.63		13.88±2.93				
	FL steps	34.44±4.36		30.44±3.84		30.76±3.83		33.94±4.40				
	HL steps	31.06±2.95		29.81±3.00		8.18±1.59*		6.75±1.47*				
	Groom	21.46±2.49		20.46±2.90		10.23±1.65*		10.41±1.21*				
Olfaction	Visible		6.68±1.11		10.14±1.35		14.83±4.66 <sup>†</sup>		12.16±2.05			
Olfaction test performance	Trial		1		2		3		4		5	
AT2101 3-on/4-off	-	+	-	+	-	+	-	+	-	+	-	+
WT performers/n	0.89	0.88	0.89	0.81	0.67	0.75	0.89	0.88	0.94	0.94	0.94	0.94
Thy1-aSyn performers/n	0.18 <sup>†</sup>	0.44 <sup>†</sup>	0.47 <sup>†</sup>	0.38 <sup>†</sup>	0.29 <sup>†</sup>	0.63 <sup>‡</sup>	0.76	0.81	0.76	0.76	0.76	0.75

WT = wild type; FL = forelimb; HL = hindlimb; Thy1-aSyn = mice overexpressing human WT  $\alpha$ -synuclein. Pole test (time to turn, time to descend), challenging beam (time to traverse, errors per step, steps), spontaneous activity in the cylinder test (rears, FL steps, HL steps, time spent grooming), visible (surface) pellet scores, and buried pellet performance (mice that found the buried food pellet in <300 s (performers) as ratio of the total number of mice per group) in Thy1-aSyn (vehicle=18, AT2101=16) and WT (vehicle=17, AT2101=16) mice administered vehicle or AT2101 in a 3-on/4-off regimen. \* $p$ <0.01 and <sup>†</sup> $p$ <0.05 compared with the respective WT mice (2×2 analysis of variance for beam, activity, and surface pellet; one-tailed Fisher's exact test for olfaction test performance); <sup>‡</sup> $p$ <0.05 compared with vehicle control (one-tailed Fisher's exact test; mean±SEM)

**Fig. 3** AT2101 effects on nonmotor deficits (olfaction). **a** Improvement on time to find the buried food pellet on 1 out of 5 consecutive days in the 7-on/7-off regimen in WT (vehicle=16; AT2101=19) and human WT  $\alpha$ -synuclein (Thy1-aSyn) (vehicle=17; AT2101=14) male mice administered AT2101 or water. **b** Improvement on time to find the buried food pellet on 3 out of 5 consecutive days in WT (vehicle=18; AT2101=16) or Thy1-aSyn (vehicle=17; AT2101=16) mice administered AT2101 or water. \* $p$ <0.05 and \*\* $p$ <0.01, respectively, compared with wild type; # $p$ <0.05 or ##  $p$ <0.01 compared with Thy1-aSyn vehicle; <sup>o</sup> $p$ <0.05 compared with WT vehicle (mean+SEM, 2 $\times$ 5 analysis of variance followed by Bonferroni  $t$  test)



AT2101 (7-on/7-off) Administration Reduces  $\alpha$ -Synuclein Staining in Nigral Dopamine Neurons

The mechanism by which increased GCase activity might mitigate  $\alpha$ -synuclein-induced deficits in the absence of GCase mutation or insufficiency is not fully understood. One hypothesis is that lysosomal GCase may have an effect on  $\alpha$ -synuclein degradation [10]. To assess the effect of AT2101 on  $\alpha$ -synuclein levels in brain, we measured  $\alpha$ -synuclein by ELISA and immunohistofluorescence in whole-brain regions of mice administered the 7-on/7-off regimen, which has the strongest effect on motor behavior pointing to more efficient target engagement of AT2101 in this regimen; we also analyzed  $\alpha$ -synuclein levels in nigrostriatal DA neurons, which exhibit early and late dysfunction in this model [23, 24]. Neither measure was affected by drug administration (Fig. 4). However, these overall measurements include all forms of  $\alpha$ -synuclein in all cell types and may miss more localized effects. Indeed, when we measured the level of

diffuse  $\alpha$ -synuclein immunofluorescence specifically in the cytoplasm of nigrostriatal DA neurons, identified by TH immunoreactivity, with confocal microscopy we observed a significant reduction in animals that received AT2101 (7-on/7-off). Most remarkably, the very densely labeled neurons became very rare (Fig. 5a, c) as also shown by the distribution of staining intensity (Fig. 5b). Specifically, 70 % of DA neurons of mice administered 7-on/7-off AT2101 exhibited  $\alpha$ -synuclein immunofluorescence below the median level (50 %) of staining observed in mice administered vehicle (Fig. 5b). Furthermore, the number of neurons with a high  $\alpha$ -synuclein immunofluorescence level was reduced and the number of neurons with low  $\alpha$ -synuclein immunofluorescence intensity was increased in mice administered AT2101 compared with vehicle ( $p$ <0.05, bootstrapping; Fig. 5d). Thus, AT2101 seemed to affect diffuse levels of  $\alpha$ -synuclein primarily in those neurons that accumulate high levels of the protein. Although less pronounced than the overall decrease in  $\alpha$ -synuclein levels induced by overexpression of GCase in

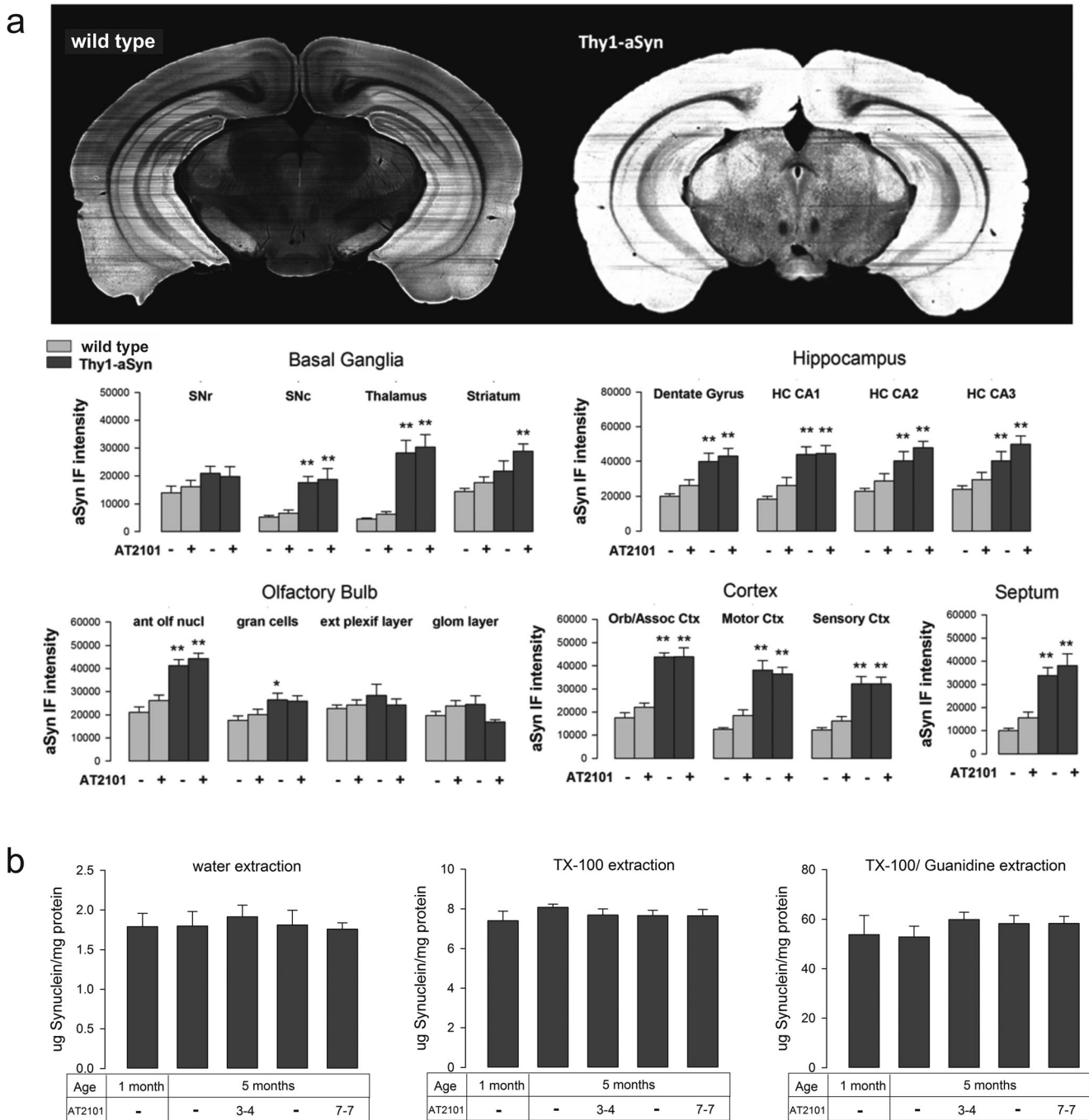


**Fig. 4** AT2101 does not change overall  $\alpha$ -synuclein protein in brain tissue. **a** Images of representative coronal sections of the substantia nigra from wild type (WT) or Thy1-aSyn mice administered vehicle illustrating increased  $\alpha$ -synuclein IF intensity in human WT  $\alpha$ -synuclein (Thy1-aSyn) mice. Administration of AT2101 in a 7-on/7-off regimen did not affect overall  $\alpha$ -synuclein immunofluorescence (IF). HC=hippocampus; ant off nucl=anterior olfactory nucleus; gran cells=granule cells; ext plexif layer=external plexiform layer; glom layer=glomerular layer; Orb/Assoc Ctx=orbital/associative cortex. \* $p < 0.05$ , \*\* $p < 0.01$

compared with the respective Thy1-aSyn mice ( $n=5$  per group,  $2 \times 2$  analysis of variance, Bonferroni  $t$  test). **b** Human  $\alpha$ -synuclein levels in brain from Thy1-aSyn mice administered AT2101 (3-on/4-off or 7-on/7-off for 4 months) or drinking water.  $\alpha$ -synuclein was extracted with water, 1 % TX-100, or 0.9 % TX-100/4.4 M Guanidine and protein quantity determined by enzyme-linked immunosorbent assay. No significant differences between vehicle and AT2101-administered groups were found (mean+SEM,  $n=6-9$ , measurements done in duplicate for each sample)

mice with *GBA1* mutations, this effect is compatible with a beneficial effect of the increased GCase activity induced by AT2101 on  $\alpha$ -synuclein levels in the neurons most affected in PD.

A major pathological consequence of the overexpression of  $\alpha$ -synuclein is the formation of intracellular aggregates. Although mouse models do not develop bona fide Lewy bodies, they show insoluble aggregates

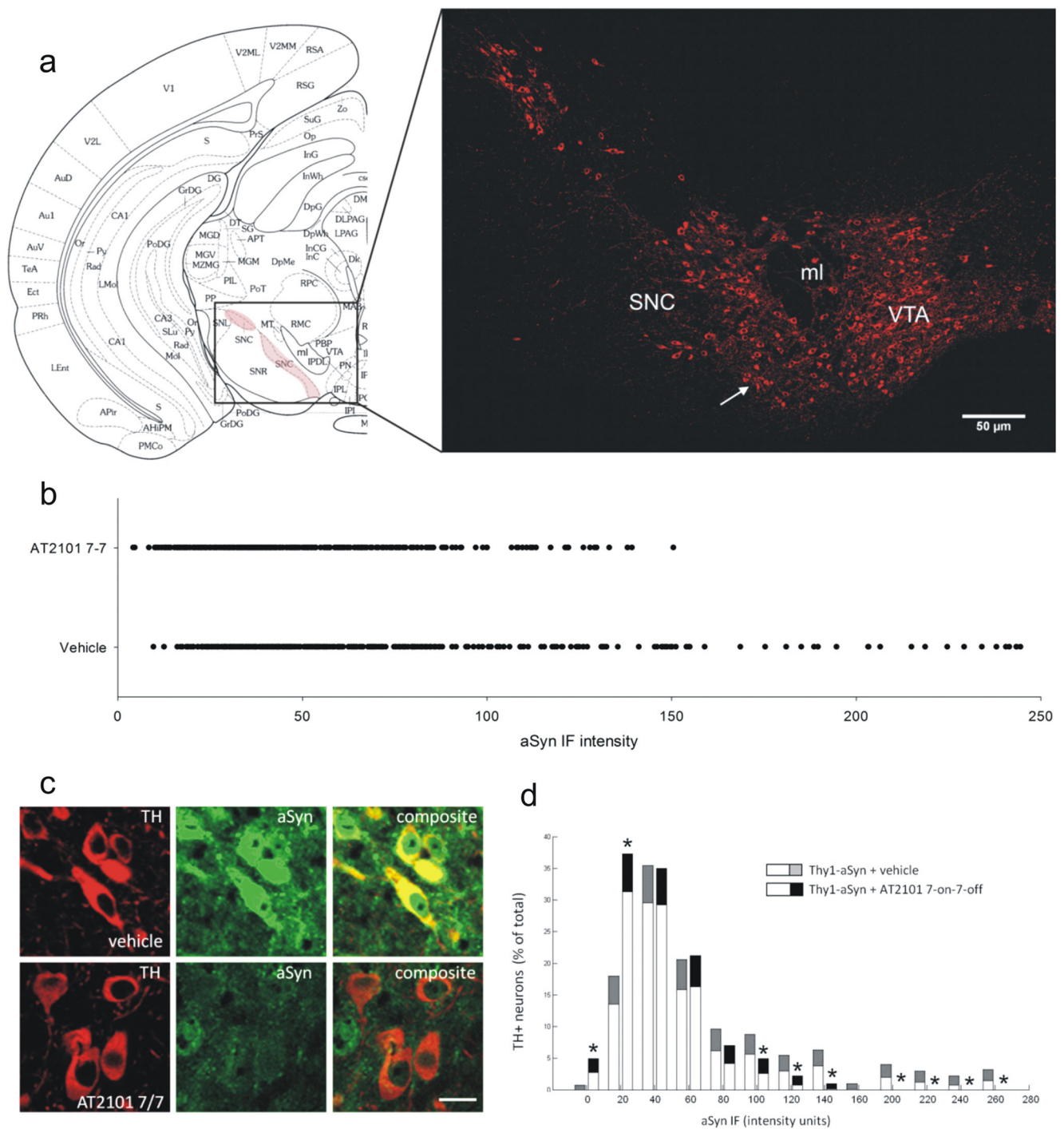


**Fig. 5** AT2101 in a 7-on/7-off regimen reduced  $\alpha$ -synuclein (aSyn) immunoreactivity in dopaminergic neurons. **a** Schematic brain section of the substantia nigra pars compacta (SNc) adapted from Paxinos and Watson [34]. The red area marks the SNc. A microscopic image (tilescan at 40-fold magnification) of a tyrosine hydroxylase (TH)-stained section is shown, the white arrow indicates the approximate location of (c) in the SNc (ml=medial lemniscus, VTA=ventral tegmental area; scale bar 50  $\mu$ m). **b** Distribution of  $\alpha$ -synuclein immunofluorescent (IF) levels of individual neurons from all mice administered vehicle or AT2101 in a 7-on/7-off (7-7) regimen. 70 % of SNc dopaminergic neurons in mice administered AT2101 exhibiting  $\alpha$ -synuclein IF below the median level of mice administered vehicle ( $\chi^2 p < 0.001$ ). **c** Images of coronal sections

of the SNc from mice over-expressing human WT  $\alpha$ -synuclein (Thy1-aSyn) mice administered vehicle or AT2101 in a 7-on/7-off regimen (scale bar is 5  $\mu$ m). Administration of AT2101 reduced  $\alpha$ -synuclein IF intensity (green) in TH-positive neurons (red) of the SNc, whereby the number of neurons with high  $\alpha$ -synuclein as shown in vehicle-treated mice is decreased after AT2101, which is shown quantitatively by the number of TH-positive neurons with different  $\alpha$ -synuclein IF levels in the bar graph. **d** Administration of AT2101 increased the number of neurons with low  $\alpha$ -synuclein IF intensity and decreased the number of neurons with high  $\alpha$ -synuclein IF intensity (means+95 % confidence intervals,  $*p < 0.05$ , bootstrapping analysis,  $n = 5$  per group). TH immunofluorescence was not changed by AT2101 administration

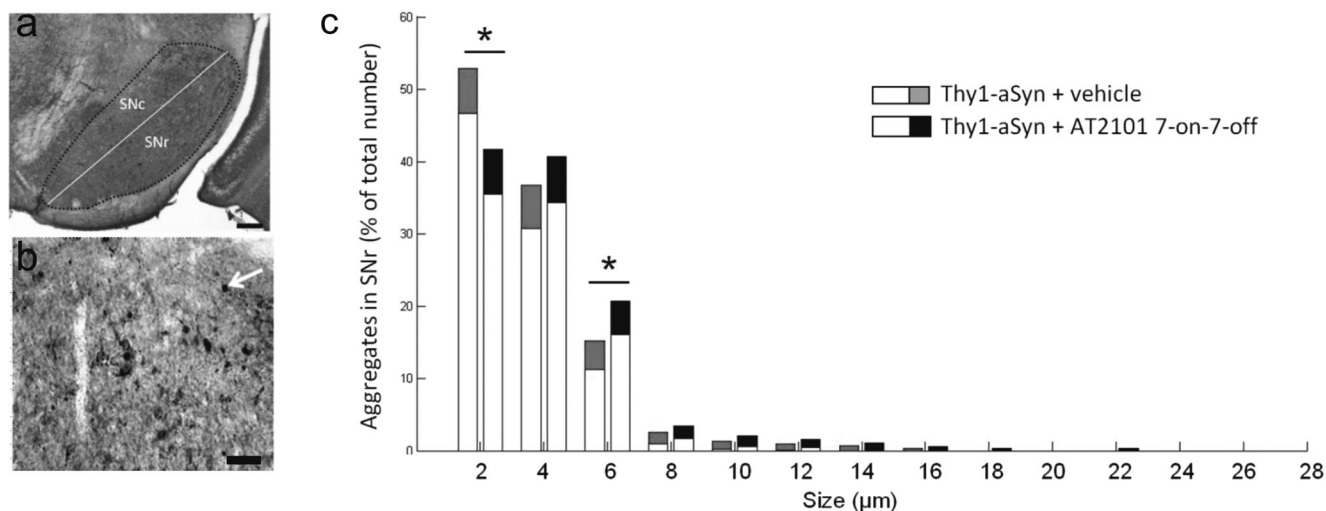


**Fig. 6** AT2101 7-on/7-off effects on  $\alpha$ -synuclein aggregates in the substantia nigra (SN.) **a** Photomicrograph of  $\alpha$ -synuclein-stained coronal section; the dotted line encloses the SN separated into the SN pars compacta (SNc) and the SN pars reticulata (SNr), scale bar 100  $\mu$ m. **b**

Photomicrograph at high magnification for quantification of  $\alpha$ -synuclein aggregates (arrow, scale bar 40  $\mu$ m). **c** Distribution of aggregate size in the SNr in mice administered vehicle or AT2101. \* $P < 0.05$  (mean + 95 % confidence intervals, bootstrapping analysis,  $n = 4-5$  per group)

of  $\alpha$ -synuclein in sections treated with proteinase K. Whether these aggregates cause deficits in neurons or represent a sink for misfolded protein and are protective, as proposed for other neurodegenerative diseases, is not clear. We measured aggregate numbers and the total area occupied by aggregated  $\alpha$ -synuclein (a proxy for aggregate size) in the dorsal (pars compacta) and the ventral (pars reticulata) SN; the latter contains a dense network of dendrites from the nigrostriatal DA neurons (Fig. 6a,b). It should be noted that the need to use proteinase K treatment to identify insoluble  $\alpha$ -synuclein aggregates precludes the identification of their specific location within cells as markers such as TH are destroyed by the treatment. No changes were observed in the dorsal SN (not shown) but the surface area occupied by aggregates increased in ventral SN of mice administered 7-on/7-off AT2101 without increase in aggregate numbers (Table 5). This suggests that AT2101 increases the number of larger aggregates, an effect confirmed by bootstrapping analysis of aggregate size

distribution (Fig. 6c). Thus, in addition to decreasing the level of cytoplasmic  $\alpha$ -synuclein immunoreactivity in highly expressing DA neurons, AT2101 leads to the formation of larger insoluble aggregates of  $\alpha$ -synuclein. The combination of these changes may explain why overall measurements of  $\alpha$ -synuclein protein by ELISA or immunohistochemistry did not detect drug effects.

#### AT2101 Reduces the Number of Activated Microglia in the SN

To determine whether AT2101 decreased inflammatory processes in the transgenic mice, we examined the distribution of microglial morphology identified by immunostaining for the microglial marker IBA-1 in the SN (Fig. 7). Based on our observations and those of others [35], resting microglia (Fig. 7a) have a diameter ranging from 1 to 4  $\mu$ m, and activated microglia (Fig. 7b) have diameters > 6  $\mu$ m. The use of 7-on/7-off AT2101 decreased microglial activation in Thy1-aSyn mice compared with vehicle. Specifically, AT2101 decreased the percentage of activated microglia and increased the percentage of resting microglia in Thy1-aSyn mice compared with vehicle (Fig. 7a-c) without affecting the percentage of activated microglia in WT mice (Fig. 7d). Indeed, following administration of AT2101, the percentage of activated microglia in Thy1-aSyn and WT mice was no longer different, indicating that AT2101 fully normalized microglial activation (Fig. 7e). Administration of AT2101 in the 3-on/4-off regimen also decreased microglial activation in Thy1-aSyn mice compared with vehicle controls (Fig. 7f); indeed, the percentage of activated microglia in Thy1-aSyn and WT mice were no longer different.

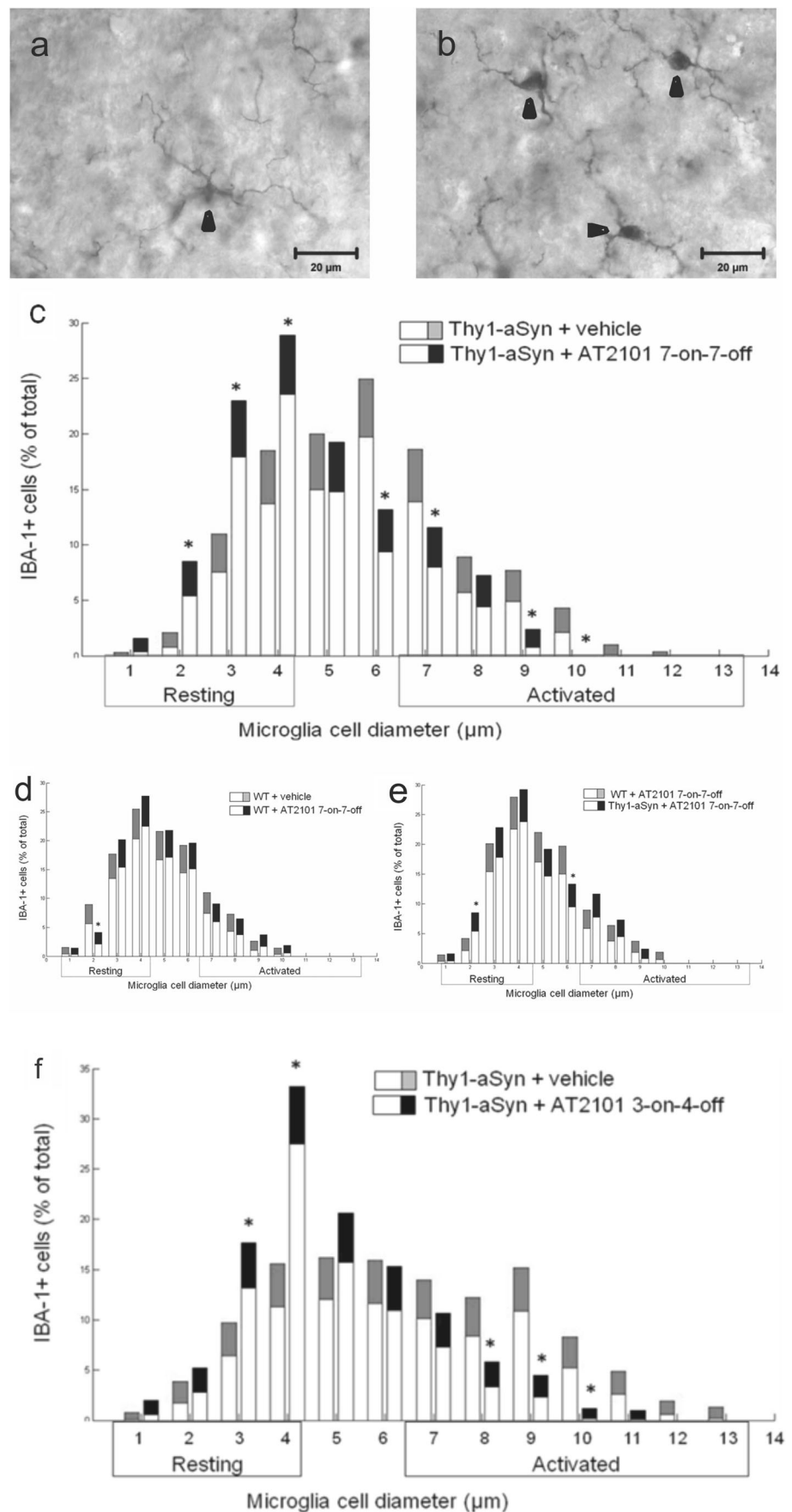
A qualitative assessment of glial fibrillary acidic protein-positive astrocytes in the SN revealed no differences between

**Table 5** Effects of AT2101 7-on/7-off on  $\alpha$ -synuclein aggregation in the pars reticulata of the substantia nigra (SNr)

Thy1-aSyn	Vehicle	AT2101
Number of aggregates	1.57 ± 0.20	2.05 ± 0.16*
Surface area occupied by aggregates	0.57 ± 0.05	0.65 ± 0.32

Thy1-aSyn = mice over-expressing human WT  $\alpha$ -synuclein. Number of proteinase K-resistant  $\alpha$ -synuclein aggregates (n/area, area in  $\mu\text{m}^2 \times 100$ ) and percentage surface area (% of area in  $\mu\text{m}^2$ ) occupied by these aggregates within the SNr in male Thy1-aSyn mice administered vehicle ( $n = 4$ ) or AT2101 ( $n = 5$ ). \*  $p < 0.05$  compared with vehicle treated-mice (mean ± SEM, 2 × 2 analysis of variance, Bonferroni  $t$  test)

**Fig. 7** AT2101 reduced microglia activation in the substantia nigra (SN). Percentage of IBA-1-positive microglia with a diameter of 1–4  $\mu\text{m}$  (resting), 5–6  $\mu\text{m}$  (hyper-ramified/partially activated), or 7–13  $\mu\text{m}$  (activated) are shown for human wild-type (WT)  $\alpha$ -synuclein (Thy1-aSyn) mice administered vehicle or AT2101. **a** Resting microglia (arrow head) in Thy1-aSyn mice administered AT2101. **b** Activated microglia (arrow heads) in Thy1-aSyn mice administered vehicle. **c** Administration of AT2101 7-on/7-off reduced the percentage of activated and increased percentage of resting microglia in Thy1-aSyn mice with **(d)** only a slight effect on resting microglia in WT mice. **e** Activated microglia are no longer increased in Thy1-aSyn mice compared with WT after administration of AT2101 7-on/7-off. **f** AT2101 3-on/4-off also reduced the percentage of activated while increasing the percentage of resting microglia (mean+95 % confidence intervals; \* $P < 0.05$ , bootstrapping,  $n = 5$  per group, scale bars are 20  $\mu\text{m}$ )



WT and Thy1-aSyn mice and no effect of AT2101 administration (not shown).

## Discussion

Enhancement of GCase by the pharmacological chaperone AT2101 ameliorated the progressive behavioral impairments and pathology observed in the Thy1-aSyn mice, a model of synucleinopathy that overexpresses human WT  $\alpha$ -synuclein. Although GCase activity is decreased in some regions of PD brains [11], and by over-expression of mutated human  $\alpha$ -synuclein in mice [36], we did not find changes in GCase activity in whole-brain extracts or lysosomally-enriched fractions from 5-month-old Thy1-aSyn mice. Thy1-aSyn mice show regionally specific pathology in the brain, with regional differences in aggregate number and sizes; and microglial activation restricted to the striatum and the SN [23, 24]. Measurements of GCase activity in different brain regions and at different ages are outside the scope of this study, but will be performed in the future in order to reveal potential GCase deficiencies. Nevertheless, these results suggest that  $\alpha$ -synuclein pathology does not generally result in a reduction of GCase activity, but requires further pathological mechanisms specific to certain brain regions and stages of progression. Accordingly, our study shows that pharmacological chaperones for GCase may be beneficial in synucleinopathies independent of the status of GCase activity, making them of potential interest for sporadic forms of PD without *GBA1* mutation.

The Thy1-aSyn mouse and most patients with PD have two WT alleles of *GBA1*. Pharmacological chaperones are able to increase the activity of both mutant and WT forms of GCase [16, 17]. If both a WT and mutant allele of *GBA1* are present, as in Gaucher carriers, chaperoning the WT protein will contribute more to the absolute increase in GCase than chaperoning the less active mutant [15]. As expected based on previous studies in mice [37, 38], 3 or 7 days of AT2101 administration followed by 1 day of washout increased the activity of WT GCase in mouse brain 1.4- or 1.8-fold, respectively. Increased GCase activity (about 1.2- to 1.3-fold) was still present after 7 days of washout, following a chronic 4-month administration. The increase in EndoH-resistant GCase protein levels after a short administration followed by 1-day washout confirmed enhanced transport of GCase to at least the cis-Golgi for glycan maturation. Thus, in the conditions of the experiment, AT2101 reached the brain and produced the expected effects of increased GCase activity and trafficking.

AT2101 administration was well tolerated in mice, and no adverse effects were observed. The mode of action of the pharmacological chaperone requires the use of alternate phases on and off drug, to allow for enzyme stabilization and activity, respectively. The optimal duration of on and off

phases must be determined empirically. Accordingly, 2 regimens were chosen for this study. The 7-on/7-off regimen likely results in stronger increase of GCase activity during the on phase compared to the 3-on/4-off regimen owing to longer duration and higher cumulative dose after 7 days compared with 3 days of administration. This was reflected in maximum effects on GCase activity after a 1-day washout (Table 2). However, differences in effects of regimens on behavior could also result from the longer period of time in which GCase is unencumbered by AT2101 inhibition. We deliberately chose to sacrifice the animals after a 7-day washout period for both regimens in order to enable direct comparison of effects on GCase activity and  $\alpha$ -synuclein pathology in the absence of high compound concentrations in brain. The results showed that both regimens induced sustained increased activity of GCase of similar magnitude; however, during drug administration, this increase would be of shorter duration in the 3-on/4-off regimen as the drug was re-administered after only 4 days off. The two regimens resulted in both similar and different effects on the various parameters examined.

Thy1-aSyn mice exhibit multiple motor and nonmotor deficits [20, 25, 39]. The reproducibility of these deficits makes Thy1-aSyn mice a robust and reliable model for long-term drug efficacy studies [23, 27, 28, 40]. Thy1-aSyn mice develop manifest parkinsonism with loss of striatal dopamine and L-dopa-responsive deficits at 14 months of age [22]. At 1–5 months of age, as used in this study, Thy1-aSyn mice represent a model of early, premanifest PD. The 7-on/7-off regimen produced significant improvement of motor deficits related to fine motor control and balance, on the pole and beam tests, without improving the decreased use of hind limb in the cylinder. The neuronal mechanisms underlying each aspect of motor deficit in mice overexpressing  $\alpha$ -synuclein is not known and may involve different CNS regions or be established at different times in the life of the animal, making them more or less amenable to improvement. Regional differences in sensitivity to level and duration of increased GCase activity, and its effect on  $\alpha$ -synuclein, may also explain why the 3-on/4-off regimen that has less effect on motor deficits than 7-on/7-off administration has a much more pronounced effect on olfactory deficits. It is not practical to measure GCase activity, trafficking, and their effects on  $\alpha$ -synuclein in multiple brain regions after different regimens and at different ages in the mice; however, the  $\alpha$ -synuclein-dependent dysfunctions in motor control and olfaction present an *in vivo* pharmacodynamic response to the changes in GCase activity and trafficking achieved with AT2101, providing a proof-of-principle for drug efficacy at a mechanistic level [23, 24].

Because mice were sacrificed 7 days after cessation of drug administration, pathology was determined at a time point when GCase activity was only increased by about 20–30 % compared with 40–80 % after 1 day of washout. Importantly, both regimens had induced a sustained reduction of



inflammatory microglial activation, a hallmark of neuropathology; however, our approach may have underestimated effects on some pathology in our model, such as overall accumulation of  $\alpha$ -synuclein in brain, which was unchanged by AT2101 after 7-day washout. This global measure may also overlook effects on soluble  $\alpha$ -synuclein. Indeed, we detected a reduction of  $\alpha$ -synuclein immunoreactivity in DA neurons, which may be due to a sustained effect on  $\alpha$ -synuclein clearance in these neurons. Administration of AT2101 also reduced the number of small  $\alpha$ -synuclein aggregates while increasing the number of large aggregates in the SN. There is ample evidence that small presynaptic  $\alpha$ -synuclein aggregates may be toxic and impair neuronal function, whereas large aggregates in the soma of neurons could be innocuous or protective [41–43]. The impact of the dosing regimen on the outcome of GCCase enhancement suggests that other regimens with AT2101 or administration of other pharmacological chaperones with different pharmacokinetics could further improve the effect of GCCase chaperoning on  $\alpha$ -synuclein accumulation.

In summary, administration of AT2101 in Thy1-aSyn mice improved motor performance, reduced inflammatory microglial activation, and reduced  $\alpha$ -synuclein immunoreactivity in nigral DA neurons. Thus, the enhancement of GCCase activity by AT2101 may have improved  $\alpha$ -synuclein clearance in DA neurons by lysosomal degradation mechanisms [44], which is in agreement with the current hypothesis of GCCase and  $\alpha$ -synuclein interaction [6, 7, 14]. Reduction of  $\alpha$ -synuclein burden in DA neurons and a decrease in the number of small  $\alpha$ -synuclein aggregates in subregions of the SN, in the context of decreased inflammation and behavioral improvements support a beneficial effect of AT2101 in Thy1-aSyn mice. Our results support that lysosomal function and, in particular, lysosomal GCCase activity, is a promising target for addressing the manifestation of synucleinopathies, even in the absence of a Gaucher mutation. These results support further development of pharmacological chaperones for GCCase for *GBA1*-associated PD, sporadic PD, and other synucleinopathies.

**Acknowledgments** This work was supported by Amicus Therapeutics, Inc., the UCLA Morris K. Udall Parkinson Disease Research Center of Excellence (PHS grant NS-P50 NS38367), and gifts to the Center for the Study of Parkinson's Disease at UCLA. We thank Dr. Alan Garfinkel, UCLA, for help with statistical analyses, and Fabrice Cordelières, CNRS France, for providing the protocol on confocal tile scan imaging. Confocal laser scanning microscopy was performed at the California NanoSystems Institute (CNSI) Advanced Light Microscopy/Spectroscopy Core Laboratory at UCLA, supported by funding from a NSF Major Research Instrumentation grant (CHE-0722519). MFC has received honoraria and travel reimbursement from the Michael J. Fox Foundation. LP, BR, RK, JF, DJL, BAW, and SWC are employees of Amicus Therapeutics. BW is the author of 2 patents that are related to this work. The authors have no additional financial interests.

**Required Author Forms** Disclosure forms provided by the authors are available with the online version of this article.

## References

- Hardy J. Genetic analysis of pathways to Parkinson disease. *Neuron* 2010;68:201–216.
- Pankratz N, Nichols WC, Elsaesser VE, P et al. Alpha-synuclein and familial Parkinson's disease. *Mov Disord* 2009;24:1125–1131.
- Trojanowski JQ, Lee VM. Parkinson's disease and related alpha-synucleinopathies are brain amyloidoses. *Ann N Y Acad Sci* 2003;991:107–110.
- Bultron G, Kacena K, Pearson D, et al. The risk of Parkinson's disease in type 1 Gaucher disease. *J Inher Metab Dis* 2010;33:167–173.
- Sidransky E, Nalls MA, Aasly JO, et al. Multicenter analysis of glucocerebrosidase mutations in Parkinson's disease. *N Engl J Med* 2009;361:1651–1661.
- Cookson MR. A feedforward loop links Gaucher and Parkinson's diseases? *Cell* 2011;146:9–11.
- Dawson TM, Dawson VL. A lysosomal lair for a pathogenic protein pair. *Sci Transl Med* 2011;3:91ps28.
- Mazzulli JR, Xu YH, Sun Y, et al. Gaucher Disease Glucocerebrosidase and alpha-Synuclein Form a Bidirectional Pathogenic Loop in Synucleinopathies. *Cell* 2011;146:37–52.
- Yap TL, Velayati A, Sidransky E, Lee JC. Membrane-bound alpha-synuclein interacts with glucocerebrosidase and inhibits enzyme activity. *Mol Genet Metab* 2013;108:56–64.
- Yap TL, Gruschus JM, Velayati A, et al. Alpha-synuclein interacts with Glucocerebrosidase providing a molecular link between Parkinson and Gaucher diseases. *J Biol Chem* 2012;286:28080–28088.
- Gegg ME, Burke D, Heales SJ, et al. Glucocerebrosidase deficiency in substantia nigra of parkinson disease brains. *Ann Neurol* 2012;72:455–463.
- Cullen V, Sardi SP, Ng J, et al. Acid beta-glucosidase mutants linked to Gaucher disease, Parkinson disease, and Lewy body dementia alter alpha-synuclein processing. *Ann Neurol* 2011;69:940–953.
- Sardi SP, Clarke J, Kinnecom C, et al. CNS expression of glucocerebrosidase corrects alpha-synuclein pathology and memory in a mouse model of Gaucher-related synucleinopathy. *Proc Natl Acad Sci U S A* 2011;108:12101–12106.
- Schapiro AH, Gegg ME. Glucocerebrosidase in the pathogenesis and treatment of Parkinson disease. *Proc Natl Acad Sci U S A* 2013;110:3214–3215.
- Valenzano KJ, Khanna R, Powe AC, et al. Identification and characterization of pharmacological chaperones to correct enzyme deficiencies in lysosomal storage disorders. *Assay Drug Develop Technol* 2011;9:213–235.
- Khanna R, Benjamin ER, Pellegrino L, et al. The pharmacological chaperone isofagomine increases the activity of the Gaucher disease L444P mutant form of beta-glucosidase. *FEBS J* 2010;277:1618–1638.
- Stee RA, Chung S, Wustman B, Powe A, Do H, Kornfeld SA. The iminosugar isofagomine increases the activity of N370S mutant acid beta-glucosidase in Gaucher fibroblasts by several mechanisms. *Proc Natl Acad Sci U S A* 2006;103:13813–13818.
- Ron I, Horowitz M. ER retention and degradation as the molecular basis underlying Gaucher disease heterogeneity. *Hum Mol Genet* 2005;14:2387–2398.
- Sawkar AR, Schmitz M, Zimmer KP, et al. Chemical chaperones and permissive temperatures alter localization of Gaucher disease associated glucocerebrosidase variants. *ACS Chem Biol* 2006;1:235–251.
- Fleming SM, Salcedo J, Fernagut PO, et al. Early and progressive sensorimotor anomalies in mice overexpressing wild-type human alpha-synuclein. *J Neurosci* 2004;24:9434–9440.

21. Rockenstein E, Mallory M, Hashimoto M, et al. Differential neuropathological alterations in transgenic mice expressing alpha-synuclein from the platelet-derived growth factor and Thy-1 promoters. *J Neurosci Res* 2002;68:568–578.
22. Lam HA, Wu N, Cely I, et al. Elevated tonic extracellular dopamine concentration and altered dopamine modulation of synaptic activity precede dopamine loss in the striatum of mice overexpressing human alpha-synuclein. *J Neurosci Res* 2011;89:1091–1102.
23. Chesselet MF, Richter F. Modelling of Parkinson's disease in mice. *Lancet Neurol* 2011;10:1108–1118.
24. Chesselet MF, Richter F, Zhu C, Magen I, Watson MB, Subramaniam SR. A progressive mouse model of Parkinson's disease: the Thy1-aSyn ("Line 61") mice. *Neurotherapeutics*. 2012;9:297–314.
25. Fleming SM, Tetreault NA, Mulligan CK, Hutson CB, Masliah E, Chesselet MF. Olfactory deficits in mice overexpressing human wildtype alpha-synuclein. *Eur J Neurosci* 2008;28:247–256.
26. Fernagut PO, Hutson CB, Fleming SM, et al. Behavioral and histopathological consequences of paraquat intoxication in mice: effects of alpha-synuclein over-expression. *Synapse* 2007;61:991–1001.
27. Fleming SM, Mulligan CK, Richter F, et al. A pilot trial of the microtubule-interacting peptide (NAP) in mice overexpressing alpha-synuclein shows improvement in motor function and reduction of alpha-synuclein inclusions. *Mol Cell Neurosci* 2011;46:597–606.
28. Richter F, Gao F, Medvedeva V, et al. Chronic administration of cholesterol oximes in mice increases transcription of cytoprotective genes and improves transcriptome alterations induced by alpha-synuclein overexpression in nigrostriatal dopaminergic neurons. *Neurobiol Dis* 2014;69C:263–275.
29. Lu XH, Fleming SM, Meurers B, et al. Bacterial artificial chromosome transgenic mice expressing a truncated mutant parkin exhibit age-dependent hypokinetic motor deficits, dopaminergic neuron degeneration, and accumulation of proteinase K-resistant alpha-synuclein. *J Neurosci* 2009;29:1962–1976.
30. Watson MB, Richter F, Lee SK, et al. Regionally-specific microglial activation in young mice over-expressing human wildtype alpha-synuclein. *Exp Neurol* 2012;237:318–334.
31. Efron B, Tibshirani R. Statistical data analysis in the computer age. *Science* 1991;253:390–395.
32. Watson JB, Hatami A, David H, et al. Alterations in corticostriatal synaptic plasticity in mice overexpressing human alpha-synuclein. *Neuroscience* 2009;159:501–513.
33. Wu N, Joshi PR, Cepeda C, Masliah E, Levine MS. Alpha-synuclein overexpression in mice alters synaptic communication in the corticostriatal pathway. *J Neurosci Res* 2010;88:1764–1776.
34. Paxinos G, Franklin KBJ. The mouse brain in stereotaxic coordinates. Academic Press, San Diego, CA, 2001.
35. Batchelor PE, Liberatore GT, Wong JY, et al. Activated macrophages and microglia induce dopaminergic sprouting in the injured striatum and express brain-derived neurotrophic factor and glial cell line-derived neurotrophic factor. *J Neurosci* 1999;19:1708–1716.
36. Sardi SP, Clarke J, Viel C, et al. Augmenting CNS glucocerebrosidase activity as a therapeutic strategy for parkinsonism and other Gaucher-related synucleinopathies. *Proc Natl Acad Sci U S A* 2013;110:3537–3542.
37. Sun Y, Liou B, Xu YH, et al. Ex vivo and in vivo effects of isofagomine on acid beta-glucosidase variants and substrate levels in Gaucher disease. *J Biol Chem* 2011;287:4275–4287.
38. Sun Y, Ran H, Liou B, et al. Isofagomine in vivo effects in a neuronopathic Gaucher disease mouse. *PLoS One* 2011;6:e19037.
39. Fleming S, Chesselet MF. Modeling non-motor symptoms of Parkinson's disease in genetic mouse models. In: Groenewegen HJ, Voorn P, Berendse HW, Mulder AB, Cools AR, (eds) *Basal ganglia IX*. Springer, New York, 2009, pp. 483–492.
40. Lee KW, Chen W, Junn E, et al. Enhanced phosphatase activity attenuates alpha-Synucleinopathy in a mouse model. *J Neurosci* 2011;31:6963–6971.
41. Kramer ML, Schulz-Schaeffer WJ. Presynaptic alpha-synuclein aggregates, not Lewy bodies, cause neurodegeneration in dementia with Lewy bodies. *J Neurosci* 2007;27:1405–1410.
42. Tompkins MM, Hill WD. Contribution of somal Lewy bodies to neuronal death. *Brain Res* 1997;775:24–29.
43. Schulz-Schaeffer WJ. The synaptic pathology of alpha-synuclein aggregation in dementia with Lewy bodies, Parkinson's disease and Parkinson's disease dementia. *Acta Neuropathol* 2010;120:131–143.
44. Martinez-Vicente M, Tallozy Z, Kaushik S, et al. Dopamine-modified alpha-synuclein blocks chaperone-mediated autophagy. *J Clin Invest* 2008;118:777–788.